J. Membrane Biol. 131, 81–92 (1993)

The Journal of
Membrane Biology

Membrane Stretch Activates a High-Conductance K^+ Channel in G292 Osteoblastic-Like Cells

Robert M. Davidson
Department of Periodontology, University of Connecticut Health Center, Farmington, Connecticut 06030

Summary. A high-conductance K^+-selective ion channel was studied in excised membrane patches from human G292 osteoblast-like osteosarcoma cells. Channel conductance averaged ~170 pS in symmetric solutions of 153 mM KCl, and ~135 pS when the pipette was filled with standard saline (150 mM NaCl). The probability of the channel being in an open state (P_{open}) increased with membrane potential, internal calcium, and applied negative pressure. At pCa7, channel activity was observed at membrane potentials greater than ~60 mV, while at pCa3, channel activity was seen at ~10 mV. Likewise, in the absence of applied pressure, channel openings were rare (P_{open} = 0.02), whereas with −3 cm Hg applied pressure, P_{open} increased to ~0.40. In each case, i.e., voltage, calcium concentration, and pressure, the increase in P_{open} resulted from a decrease in the duration of long-closed (interburst) intervals and an increase in the duration of long-open (burst) intervals. Whole-cell responses were consistent with these findings. Hypotonic shock produced an increase in the amplitude and conductance of the outward macroscopic current and a decrease in its rise time, and both single-channel and whole-cell currents were blocked by barium. It is suggested that the voltage-gated, calcium dependent maxi-K^+ channel in G292 osteoblastic cells is sensitive to membrane stretch and may be directly involved in osmoregulation of these cells. Further, stretch sensitivity of the maxi-K^+ channel in osteotrophic cells may represent an adaptation to stresses associated with mechanical loading of mineralized tissues.

Key Words Osteoblasts · ion channels · osmoregulation · mechanotransduction · stretch activation · potassium selectivity

Introduction

Mechanical stimulation of osteoblastic cells in vitro results in increased metabolic activity associated with changes in the membrane potential of these cells (Chow et al., 1984; Heath et al., 1984*a*, *b*; Edelman, Fritsch & Balsan, 1986; Ferrier & Ward, 1986; Fritsch, Edelman & Balsan, 1988; Ngan et al., 1988). The effects of mechanical stimulation on membrane potential have been viewed as largely indirect, via changes in field potential, surface charge, and/or increased release of neuropeptides, cytokines, or intracellular messengers (Pollack, Salzstein & Pienkowski, 1984; Ngan et al., 1988; Sandy et al., 1989; but *see* Rodan, 1991). Recent studies, however, show evidence for a variety of stretch-activated ion channels in bone cells (Duncan and Misler, 1989; Yamaguchi et al., 1989; Davidson, Tatakis & Auerbach, 1990), suggesting that mechanical stimulation may activate conductances in the osteoblast membrane more directly, i.e., that there exist mechanosensitive transduction mechanisms at the cellular level capable of modulating membrane potential.

Our previous studies (Davidson et al., 1990), have shown that G292 osteoblast-like cells contain at least three types of mechanosensitive ion channels; in cell-attached patches, the application of negative pressure to the recording pipette activates ionic conductances of approximately 160, 60, and 20 pS in these cells. One of these, a large-conductance (160 pS) channel that was tentatively identified as K^+ selective, showed kinetic behavior similar to that of a Ca^{2+}-activated, voltage-gated potassium channel found in osteoblastic cells (Dixon, Aubin & Dainty, 1984; Ypey et al., 1988; Ravesloot et al., 1990). Of the two remaining mechanosensitive channels, both may have been capable of increasing intracellular calcium: the 60 pS channel was rather nonselective for cations, and the 20 pS channel was similar in conductance properties to a Ca^{2+}-conducting cation channel found in UMR-106 osteoblastic cells (Duncan & Misler, 1990). If the 160 pS channel was calcium dependent, increased channel activity could have been the result of an increase in internal calcium mediated by one or both of these smaller-amplitude mechanosensitive channels (Sackin, 1989; Ubl, Murer & Kolb, 1988; Taniguchi & Guggino, 1989). Although stretch-induced activity of the 160 pS channel was recorded in the absence of extracellular calcium, the possibility remained that membrane de-

Table. Summary of solutions

	NaCl	KAc	NaAc	KCl	$CaCl_2$	$MgCl_2$ (in mM)	EGTA	HEPES	pCa	$BaCl_2$	Sucrose	mOsm
Single-Channel Recordings												
ECS	150			3	1	1	1	10	5			
ECS-acetate		3	150		1	1	1	10	5			
ICS-acetate		153			1	1	1	10	5			
ICS-3				153	2	2	1	10	3			
ICS-4				153	0.2	2	0.1	10	4			
ICS-5				153	1	2	1	10	5			
ICS-6				153	1.9	2	2	10	6			
ICS-7				153	1.25	2	2	10	7			
ICS-8				153	0.25	2	2	10	8			
Whole-Cell Recordings												
ICS-Ca^{2+}-free				153		2	0.1	10				292
ECS-isotonic	148			5	1.75	2	1	10				297
ECS-hypotonic	74			2.5	1.75	2	1	10				214
Reduced isotonic	74			2.5	1.75	2	1	10			152	301
Barium hypotonic				2.5	0.5			10		70		220

formation elevated internal calcium levels (Snowdowne, 1987).

One of the objectives in the present study was to determine whether the 160 pS ion channel found in G292 osteoblasts was of the same class of large-conductance K^+ channel found in osteoblastic cells (Dixon et al., 1984; Ypey et al., 1988; Ravesloot et al., 1990). In these experiments, it was important to more clearly establish the ion selectivity, conductance, gating, and general kinetic properties of this channel. A second objective was to determine if the activity of the 160 pS channel could be modulated by membrane stretch, independent of changes in voltage or internal calcium concentration. Accordingly, the excised patch (Hamill et al., 1981) was used to examine the conductance, selectivity, kinetic behavior, and pressure sensitivity of this channel while calcium concentration on both sides of the patch was well controlled. In a second series of experiments, single channel findings were confirmed by recording stretch-induced macroscopic currents in the whole-cell mode.

Materials and Methods

Human osteoblast osteosarcoma G292 (#CRL 1423) cells were obtained from American Type Culture Collection (Rockville, MD) and maintained at 37°C with McCoy's 5a supplemented with 5% or 10% fetal calf serum, penicillin, and streptomycin in a 5% CO_2 humidified incubator. These cells were chosen because of their well-characterized osteoblast-like phenotype (Peebles, Trisch & Papageorge, 1978; Shupnik & Tashjian, 1982). Cells of early passage were seeded at 2.5×10^4 cells/ml (1 ml/dish; 35-mm dishes), and then incubated for two to six days. In several experiments, cells were grown on glass coverslips, and then transferred to a perfusion chamber.

For single channel studies, pipette and recording media consisted of either standard extracellular saline (ECS) or a potassium-rich intracellular (ICS) solution (*see* Table for a summary of all solutions).

Patches were in the excised, outside-in configuration (but *see* Fig. 9*C*); pipette resistances ranged from 4 to 12 MΩ, and high-resistance seals ranged from ~5–50 GΩ. To rule out possible confounding effects of chloride conductances found in osteoblastic cells (Chesnoy-Marchais & Fritsch, 1989; Ravesloot et al., 1991), in a number of experiments acetate was substituted for chloride in both pipette and bath solutions. For these recordings, there were no significant differences in channel conductance or selectivity for potassium (*see* Fig 1), and data were pooled with recordings obtained in chloride salts.

For current-voltage relationships, command potentials were applied stepwise to the pipette in 5 or 10 mV intervals, typically over a 50–75 mV range. Data record length depended on the activity of the channel, i.e., number of events, but typically ranged from 40 to 90 sec at each voltage step. For ion selectivity and calcium dependence studies, conventional ion substitution paradigms were followed. Pressure, expressed as cm Hg (suction negative), was applied through the pipette using a 20-cc syringe, and monitored with a mercury manometer in parallel with the pipette. Pressure was usually applied in 0.5 cm Hg increments (~2–3 sec/pressure step), and data sets ranged in length from 45 to 320 sec. Pressure was applied until the patch ruptured, typically −4.0 to −4.5 cm Hg.

Single-channel currents were monitored with an Axopatch 1-C (Axon Instruments, Foster City, CA) and stored on tape using a conventional VHS video recorder and a modified digital audio processor (Sony PCM-701ES, Tokyo, Japan). For kinetic analyses, analog signals were filtered with an 8-pole low-pass Bessel filter (Frequency Devices, Haverhill, MA) at a cut-off

frequency of 0.5 or 3 kHz and digitized at a sampling rate of 1 or 10 kHz using pCLAMP (Axon Instruments, Foster City, CA). Single channel currents were detected by additional automated analysis programs (IPROC and LPROC, Axon Instruments, Foster City, CA), and data sets were fitted by appropriate functions with a nonlinear least-square algorithm (NFITS, C. Lingle, Washington Univ., St. Louis, MO). For interval duration histograms, the residuals were weighted by the inverse of the number of counts in each bin; for all other datasets, uniform weighting was used. Frequency histograms of current amplitude were fitted by sums of Gaussians, and mean current amplitudes and the probabilites of a single channel being open (P_{open}) were derived from the fitted values (Yang, 1989):

$$P_{open} = 1 - P_{closed}^{1/n}, \quad (1)$$

where P_{closed} is the probability of not being open in the record (equal to the number of samples in the baseline peak divided by the total samples in the record), and n is the number of channels in the patch, taken as the largest integral multiple of the unitary current level. For very small channel currents, or at more hyperpolarized potentials where channels were typically inactive, discrete peaks in the amplitude histogram were not always apparent, and the current amplitude was estimated as the mean amplitude of manually detected single channel currents. Reversal potentials were obtained either by interpolation or extrapolation of linear current-voltage plots using a standard linear regression analysis. Nonlinear current-voltage relationships (*see* Fig. 1*B*) and pressure sensitivity curves (*see* Fig. 4*B*) were fitted using a least-squares nonlinear regression analysis (Plot-IT, Scientific Programing, Haslett, MI).

For whole-cell studies, patch pipettes were filled with calcium-free ICS and cells were bathed in ECS or an isotonic reduced-salt solution. To alter the osmotic gradient, a hypotonic solution with reduced potassium and sodium, or barium concentration was substituted in the bath. Osmolarity was measured using a vapor-pressure osmometer (WESCOR 5100-C, Logan, Utah). For current-voltage relationships, voltage was applied using pCLAMP. Recorded currents were filtered at 1–2 KHz, and resultant current traces were fitted with a least-squares algorithm for both amplitude and time constant using pCLAMP.

In excised outside-in patches, membrane potential (V_{mem}) is defined as the negative of the pipette potential ($-V_p$), while for whole-cell and excised outside-out (*see* Fig. 9*C*) patches, V_{mem} is defined as V_p. The pH of all solutions was adjusted to 7.4, and all recordings were obtained at room temperature.

Results

The predominant cation carrier in G292 osteoblastic cells is a large conductance (~135–170 pS), voltage-sensitive K^+-selective ion channel that was present in the majority of excised patches; in the outside-in configuration, 79% (56/71) of the patches recorded in these cells contained this channel. The channel was calcium dependent, and in many cases could be activated by mechanically stretching the membrane. This channel was present in early (2–3 days) cultures and persisted in cultures that had reached confluence (7–10 days). Further, the conductance and selectivity were not significantly different between pre- and post-confluent recordings. Once cells had reached confluence, however, it was often difficult to obtain an adequate high-resistance seal, and impossible to achieve adequate whole-cell recordings. Thus, the majority of recordings were taken from cells that were in a nonconfluent state (2–6 days). Typically, patches contained ~3 channels (2.9 ± 1.3; mean ± SD; n = 28).

Ion Selectivity

Fig. 1*A* shows the typical current-voltage relationship observed, in this case with solutions of standard ECS or ECS-acetate in the recording pipette and ICS or ICS-acetate in the bath. For each of these records, the reversal potential (E_{rev}) approached −70 mV, which is consistent with a potassium-selective conductance; in ECS, E_{rev} was −61 mV, while in ECS-acetate E_{rev} was −68 mV. Moreover, slope conductances were similar, i.e., 134 pS in ECS *vs.* 127 pS in ECS-Acetate. For a total of 17 patches recorded with the ECS salt in the pipette and ICS salt in the bath, mean slope conductance was 135 ± 17 pS (Mean ± SD), and the reversal potential was −64 ± 9 mV. Inset shows channel activity in the patch recorded in ECS. The membrane potential is indicated to the left of each record, and open and closed states are indicated by the letters *o* and *c*. The patch contained two maxi-K^+ channels.

The selectivity of the channel is further illustrated in Fig. 1*B*. That this was a potassium-selective, rather than a chloride conductance was confirmed by comparing recordings obtained in symmetric solutions of ICS-acetate with recordings in an ICS-acetate gradient. In symmetric solutions (open circles), the slope conductance was linear and nonrectifying and the reversal potential, as expected, near zero (168 ± 22 pS; −4 ± 1 mV; n = 11). By contrast, after the solution in the bath was exchanged for ECS-acetate (filled circles), there was a shift to the right of the *I-V* curve towards more positive potentials. Further, it became nonlinear, and was more appropriately fit by a polynomial rather than a straight line, characteristic of the maxi-K^+ channel found in other osteogenic cells (Ravesloot et al., 1990). The ratio of potassium-to-sodium permeability (PK/PNa) was calculated using the equation:

$$E_{rev} = 25 \ln([Na]_o * (PNa/PK) + [K]_o) / ([Na]_i * (PNA/PK) + [K]_i), \quad (2)$$

where $[Na]_o$ and $[Na]_i$ are the outside (pipette) and inside (bath) concentrations of Na^+, and $[K]_o$ and

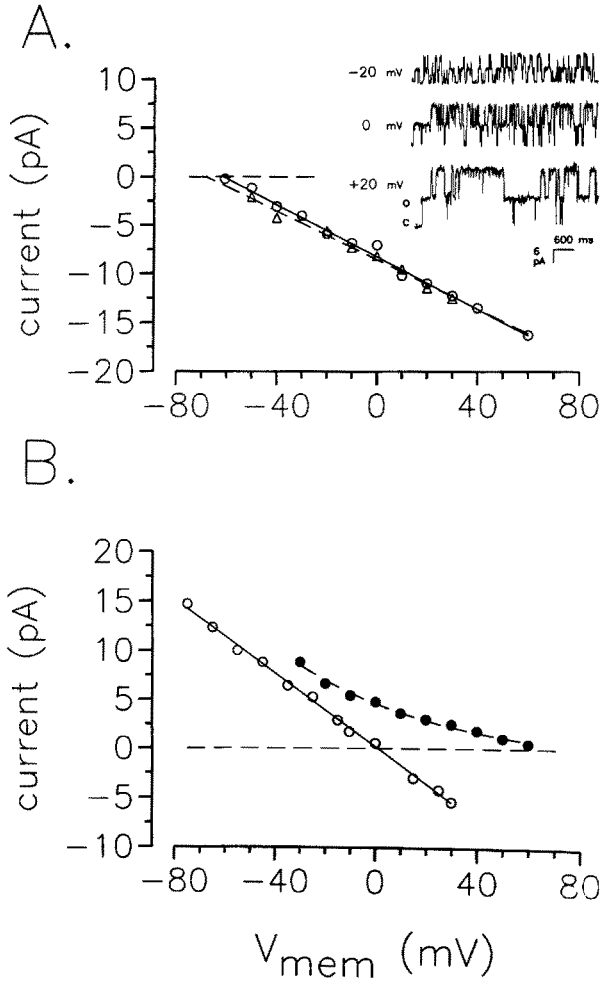

Fig. 1. Conductance and selectivity of the maxi-K^+ channel. (*A*) Current-voltage relationship of the maxi-K^+ channel recorded in ICS (open circles; solid line) and ICS acetate (filled circles; dashed line). Dashed lines represent zero current levels. Reversal potentials were obtained by extrapolation of the least-squares fit to the data points. Both cells were from 5-day cultures. Inset: single channel activity in an excised, outside-in patch at −20 mV (top trace), 0 mV (middle trace), and 20 mV (bottom trace). Outward (negative) currents are shown as upward deflections. (*B*) Current-voltage relationships for maxi-K^+ channels in symmetric ICS acetate (open circles) and ECS acetate (filled circles). After substituting ECS acetate in the bath, E_{rev} shifted to ~72 mV. The cell was from a 4-day culture.

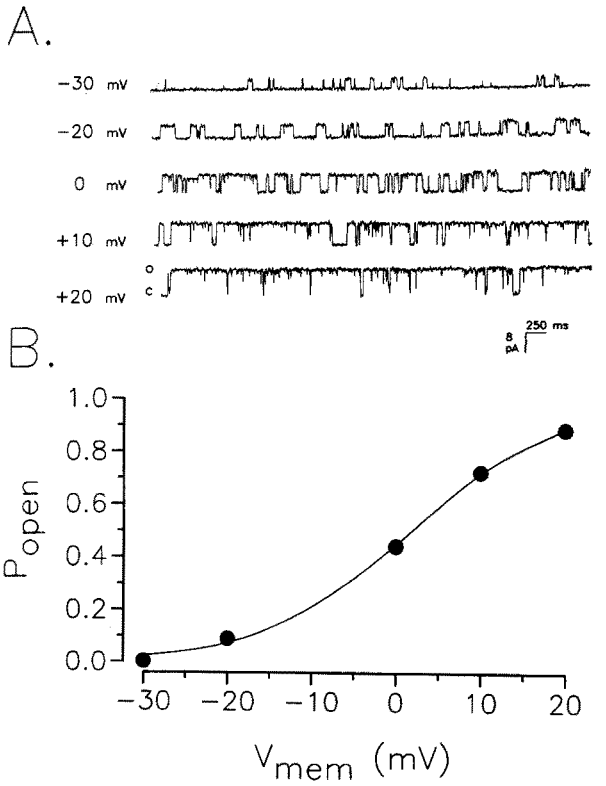

Fig. 2. Voltage dependence of the maxi-K^+ channel activation. (*A*) Single-channel currents in an excised, outside-in patch containing a single maxi-K^+ channel; membrane potential is indicated to the left of each trace. P_{open} increased from 0.04 at −30 mV to 0.91 at 20 mV. Record lengths ranged from 49 to 243 sec. E_{rev} was −70 mV and channel conductance was 123 pS. Pipette: ECS; Bath: ICS (pCa4). The cell was from a 6-day culture. (*B*) P_{open}-voltage relationship for data record in *A*; solid line represents a fit of the data points to a Boltzmann equation (*see text*). The channel reached half-maximum P_{open} ($V_{.5}$) at a membrane potential of 2 mV.

$[K]_i$ are the outside and inside concentrations of K^+, respectively. With ICS in the bath and ECS in the pipette, the ratio was 13 ± 4 (n = 17).

Voltage Dependence

As illustrated in Fig. 2*A* and *B*, the channel was also dependent on membrane voltage. That is, the probability of the channel being in an open, conducting state (P_{open}) increased as a function of membrane potential. For this and subsequent analyses (*see* Figs. 3 and 4), channel amplitude, number of channels, and P_{open} were estimated from amplitude histograms (*see* Materials and Methods: Eq. (1)). Fig. 2*A* shows a series of records obtained with ECS in the pipette and ICS in the bath. As voltage became more positive, both channel amplitude and P_{open} increased: at −30 mV the amplitude of the channel was 4.8 pA, and only a few, brief channel openings were seen, while at 20 mV, P_{open} increased to 0.91 and mean channel amplitude to 11.6 pA.

Fig. 2*B* shows a Boltzmann function that was fitted to the data points from the record in Fig. 2*A* of the form:

$$P_{open} = 1/(1 + \exp(-(V_{mem} - V_{.5})/A)), \quad (3)$$

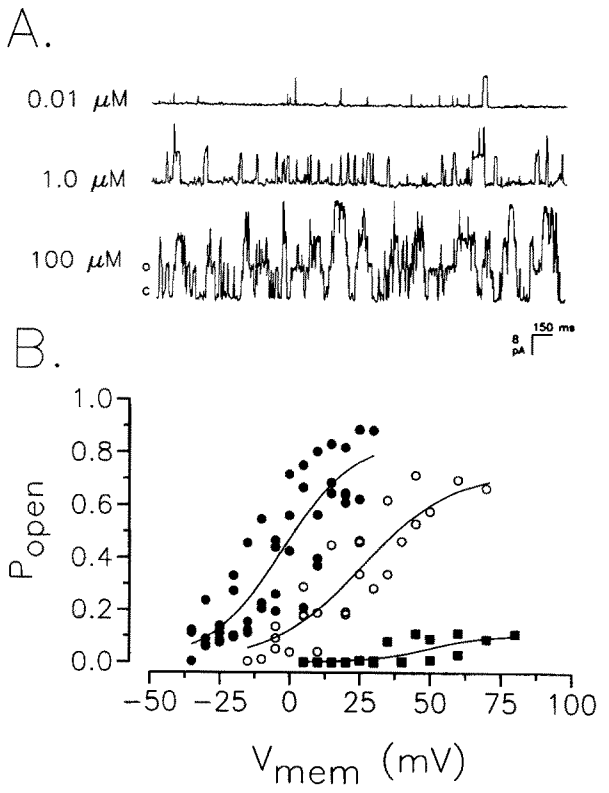

Fig. 3. Calcium dependence of the maxi-K$^+$ channel (*A*) Increasing calcium concentration in the bath increased P_{open} of the channel in an excised, outside-in patch. Top trace (213 sec total record): $P_{open} < 0.01$ (pCa8); middle trace (81 sec): $P_{open} = 0.04$ (pCa6); bottom trace (63 sec): $P_{open} = 0.37$ (pCa4). The membrane potential was held at 10 mV. Conductance of the cell was 132 pS, and the E_{rev} was −67 mV. Pipette: ECS; Bath: ICS (pCa as indicated). The cell was from a 2-day culture. (*B*) Relationship between voltage, calcium, and P_{open}. Boltzmann equations were fitted to pooled data for three ranges of internal calcium concentrations (*see text*): pCa3–4 (filled circles); pCa5–6 (open circles); pCa7–8 (squares). Pipette: ECS; Bath: ICS (pCa as indicated).

where P_{open} is the probability of the channel being in an open state, V_{mem} is the membrane potential, $V_{.5}$ the voltage at half-maximum P_{open}, and A, a slope factor. For these data, $V_{.5}$ equaled 2 mV and A was 8.9.

Calcium Dependence

The calcium dependence of the channel was studied by exposing the patch to a range of internal calcium concentrations, and Fig. 3*A* shows the effect of changes in calcium levels on the P_{open} of a patch which contained four separate maxi-K$^+$ channels. For these recordings, membrane potential was held constant at 10 mV, and the calcium concentration of the bath, indicated to the left of each trace, was changed by perfusion.

With 0.01 μM calcium in the bath (Fig. 3; top trace), channel openings were both rare and brief, and separated by long periods of inactivity ($P_{open} < 0.01$). With calcium concentration increased to 1.0 μM (middle trace), channel activity increased ($P_{open} = 0.04$), the baseline became somewhat noisier, and a second maxi-K$^+$ channel appeared. After calcium concentration was increased to 100 μM (bottom trace), there was a ~10-fold increase in P_{open}, to 0.37, and at this concentration of calcium, three levels of channel activity could be seen.

Fig. 3*B* shows the relationship between voltage and P_{open} at three ranges of internal calcium from 22 separate patches. Since there was some degree of variability in calcium-dependent activation among channels (*see also:* Ravesloot et al., 1990), data were partitioned into three groups; (i) pCa3–4, (ii) pCa5–6, and (iii) pCa7–8. To quantify the relationship between voltage, calcium concentration, and P_{open}, data points in each pCa range were fitted with Boltzmann equations as described above.

At each range of calcium concentration, there was an increase in P_{open} as membrane potential became more positive. For example, at pCa3–4, P_{open} increased from 0.11 ± 0.08 ($n = 4$) at −30 mV, to 0.77 ± 0.10 at 30 mV. Likewise, the channel showed a clear dependence on calcium: at a membrane potential of 20 mV, P_{open} increased from near zero at pCa7–8 to 0.63 ± 0.16 ($n = 4$) at pCa3–4. Further, $V_{.5}$ decreased from 49 mV in pCa7–8 to −1 mV in pCa3–4, although the voltage sensitivity of the channel was largely unaffected by changes in calcium. In pCa3–4, there were an *e*-fold change in P_{open} for every 22 ± 5 mV ($n = 6$), in pCa5–6, for every 21 ± 7 mV ($n = 10$), and in pCa7–8 for every 17 ± 5 mV ($n = 6$).

Sensitivity to Membrane Stretch

A second objective of this study was to establish whether the activity of the maxi-K$^+$ channel could be directly modulated by mechanical stretch, and Fig. 4*A* and *B* show the relationship between pressure, expressed as negative cm Hg, and channel activity. The records in Fig. 4*A* were obtained in symmetric solutions of ICS, membrane potential was held constant at −20 mV, and pressure was applied as indicated to the left of each trace.

In general, the G292 osteoblast membrane was somewhat fragile; in very few cases could applied pressures be increased beyond −4 to −4.5 cm Hg. Typically, pressure was applied step-wise, in 0.5 cm Hg increments, and the response of the channel

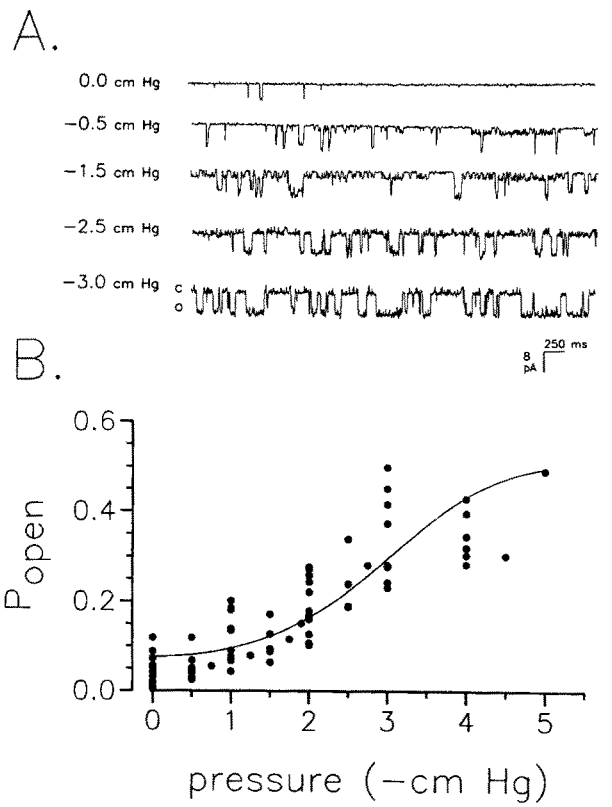

Fig. 4. Pressure dependence of the maxi-K$^+$ channel. (*A*) Single-channel activity in an excised, outside-in patch in response to applied negative pressure recorded in symmetric ICS (pCa6). Pressure (−cm Hg) indicated to the left of each trace. Membrane potential: −20 mV; Conductance: 159 pS; E_{rev}: 2 mV; Record length: 44 to 190 sec. The cell was from a 3-day culture. (*B*) P_{open} as a function of applied pressure for pooled data (n = 16) recorded under the same conditions as *A*. Data points are values for P_{open} derived from amplitude histograms, and the solid line represents a fit of the data to a Boltzmann expression which minimized the variance of the curve (*see text*); half-maximal P_{open} occurred at −2.7 cm Hg.

lagged behind the change in pressure by 2–3 seconds. As shown in Fig. 4*A*, with no applied pressure, the channel was quiescent ($P_{open} < 0.01$); in the record shown, only a few, brief channel openings can be observed. By contrast, with −0.5 cm Hg applied pressure, activity of the channel increased (P_{open} = 0.12), and a second, small amplitude (0.9 pA) channel appeared. With −3.0 cm Hg, both the frequency and duration of channel openings increased (*see* Fig. 5*C*), and the P_{open} increased to ~0.50; at this level of applied pressure most channel openings were superimposed on the ongoing activity of the smaller channel.

Overall, complete records were obtained from 16 patches tested for pressure sensitivity. There was a high degree of variability in the response of the channel to membrane tension, and this is evident in the scatter of the data points in Fig. 4*B*. A number of patches were tested at a submaximal level of applied pressure, which permitted repeated testing of the same patch. In these cases the channel showed a different kind of variability. In three patches, the channel failed to respond to membrane stretch after the first series of pressure steps. In four other patches the response to applied pressure showed hysteresis: in one patch the channel appeared more sensitive to stretch, while in the remaining three patches the channel was less sensitive to stretch and the threshold for stretch activation was elevated. In such cases, only data from the initial run was included in the analysis.

The fitted curve in Fig. 4*B* is superimposed on P_{open} data obtained from the 16 patches, and represents an estimate of the pressure sensitivity of the channel. Earlier, we found that the channel responded quite characteristically to membrane stretch (Davidson et al, 1990): (i) in the majority of patches, P_{open} plateaued, and (ii) the channel exhibited random periods of inactivity that appeared to be independent of membrane tension. In the current experiments, the channel showed similar kinetic behavior, and the same expression has been used to fit the data, albeit with some modifications to account for the differences in internal calcium levels and membrane voltage between the two series of experiments. Accordingly, the data were fitted by the following expression:

$$P_{open} = (P_{max}/(1 + K \exp(-\Theta ss P^2)) - P_{inactive}, \quad (4)$$

where P_{max} is the maximum probability of the channel being open (at pCa6, P_{max} was 0.56 ± 0.13; n = 11), $P_{inactive}$ is the probability that a channel is in an inactive state (0.05 ± 0.04; n = 16), K a slope constant, and Θss the measure of steady-state pressure sensitivity. For the records in Fig. 4*B*, the estimate of Θss was 0.18/cm^2 (5.5 cm^2 for an e-fold increase in P_{open}), which is ~40% lower than the value (0.29/cm^2) we had previously derived (Davidson et al., 1990). The difference between these two values may reflect (i) a difference in compliance of the patch in the excised *vs.* cell-attached configuration (ii) the level of control of internal calcium in the excised *vs.* cell-attached patch, or (iii) inherent variability of stretch-induced channel activity. For these data, K was 3.4.

Kinetic Analysis: What Accounts for the Change in P_{open}?

A kinetic analysis was limited to an examination of the two parameters, long-open (burst) intervals and long-closed (inter-burst) intervals, shown in cell-

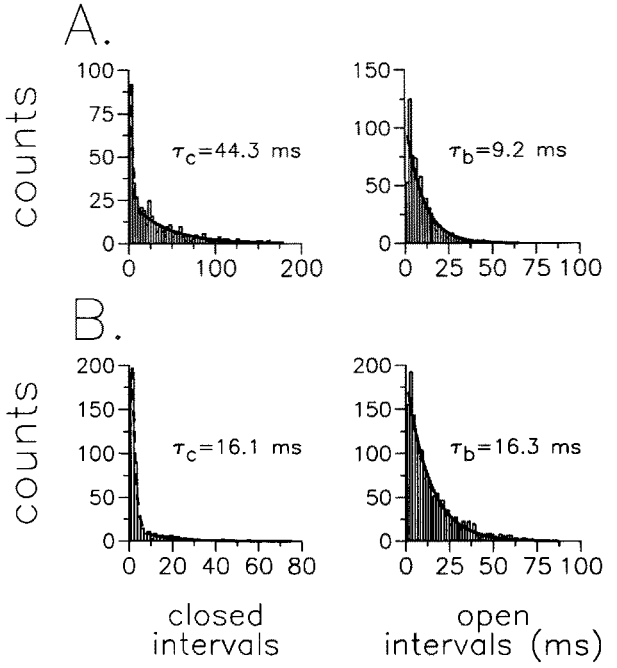

Fig. 5. Voltage dependence of closed and open interval durations. Distributions of dwell times at (*A*) −20 mV and (*B*) 10 mV for an excised, outside-in patch containing a single voltage-dependent K^+ channel. The solid lines in each distribution represent the long exponential component (τ); in each case this could be described as a single exponential. Dashed lines (*5A* and *B*; left panel) describe shorter exponential components. The duration of both long-closed (τ_c) and long-open (τ_b) intervals were sensitive to changes in voltage (*see text;* same patch as Fig. 2*A*). Record lengths ranged 66 to 201 sec and the number of events ranged from 453 to 1671.

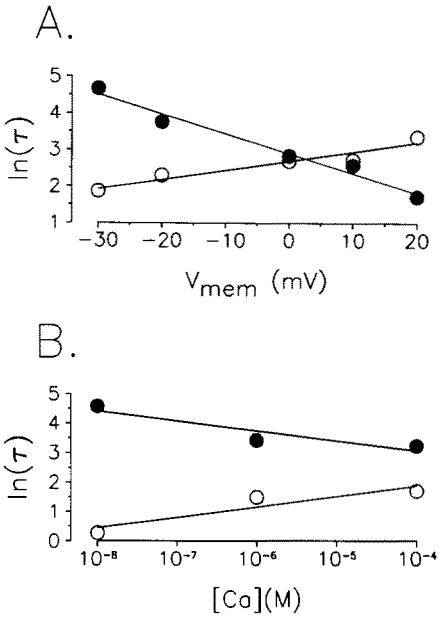

Fig. 6. (*A*) Voltage and (*B*) Calcium dependence of interval durations. Long-closed (τ_c) and long-open (τ_b) time constants could be described as single exponentials (*see* Fig. 5), and are plotted as [ln(τ)]. Solid lines in each plot represent the least-squares fit through the data points. In each case, both τ_c (filled circles) and τ_b (open circles) were sensitive to changes in the gating parameter. (*A*) (same patch as in Fig. 2*A*) τ_c decreased from 106.7 msec at −30 mV to 5.5 msec at 20 mV, while τ_b increased from 6.5 msec to 28.7 msec. (*B*) (same patch as Fig. 3*A*; at a membrane potential of 0 mV, only single-channel openings were seen). In response to a change in calcium concentration, τ_c decreased from 96.4 msec in 0.01 μM calcium to 24.8 msec in 100 μM calcium, while τ_b increased from 1.1 msec to 5.5 msec. For this analysis, record lengths ranged from 54 to 319 sec and the total number of events ranged from 305 to 4316.

attached patches to be sensitive to membrane stretch (Davidson et al., 1990).

Fig. 5*A* and *B* show the distribution of closed and open intervals at (*A*) −20 and (*B*) 10 mV for an excised patch containing a single maxi-K^+ channel, and illustrate the voltage dependence of these two kinetic parameters. The solid line in each distribution represents the long component (τ), in each case described by a single exponential; dashed segments of the fitted curves represent shorter components of the distribution not included in the analysis. In this example, the mean long-closed interval (τ_c) decreased from 44.3 msec at −20 mV (*5A*; left panel) to 16.1 msec at 10 mV (*5B*; left panel), while burst duration (τ_b) increased from 9.2 msec (*5A*; right panel) to 16.3 msec (*5B*; right panel).

Fig. 6*A* and *B* summarize the (*A*) voltage and (*B*) calcium dependence of τ_c and τ_b from two separate patches. In these examples, both τ_c and τ_b, derived from distributions of dwell times as shown above and plotted as [ln(τ)], were distributed as single exponentials. In each case there was a decrease in τ_c and an increase in τ_b with increasing voltage or calcium. As noted above, this raised the possibility that stretch-induced changes in τ_c and τ_b seen in cell-attached patches could have resulted from changes in calcium or voltage, rather than a direct effect of mechanical tension. That the two kinetic parameters were inherently sensitive to applied pressure was confirmed, however, in excised patches, and is illustrated in Fig. 7*A–C*.

In this example, mean long-closed dwell time decreased from 61.6 msec at −0.5 cm Hg applied pressure (Fig. 7*A*; left panel) to 36.1 msec at −3.0 cm Hg applied pressure (Fig. 7*B*; left panel), while τ_b increased from 5.7 (Fig. 7*A*; right panel) to 26.7 msec (Fig. 7*B*; right panel). Fig. 7*C* summarizes the pressure dependence for this channel over the range of pressure steps tested. In this case, applied negative pressure in excess of −3.0 cm Hg ruptured the patch. Two additional patches showed a similar dependence of these kinetic parameters on pressure.

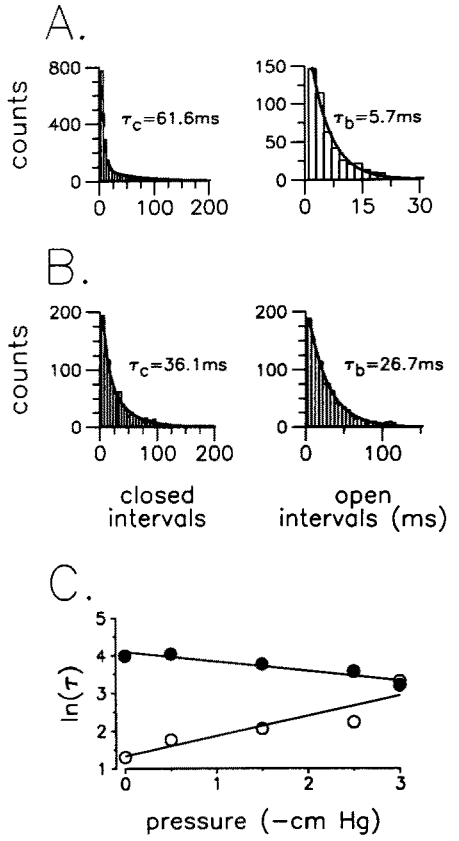

Fig. 7. Pressure dependence of interval durations. Distributions of closed and open dwell times at (*A*) −0.5 cm Hg and (*B*) −3.0 cm Hg applied pressure (same patch as Fig. 4*A*). As applied pressure was increased from −0.5 to −3.0 cm Hg, τ_c decreased from 61.6 msec to 36.1 msec and τ_b increased from 5.7 msec to 26.7 msec. (*C*) Dwell time *vs.* pressure (same convention as Fig. 6). Record lengths ranged from 44 to 190 sec and the total number of events ranged from 513 to 3325.

Hypotonic Shock Increases the Amplitude of the Macroscopic Current

Single-channel evidence notwithstanding, it was important to find out if G292 cells exhibited macroscopic mechanosensitive currents. Recent studies (Morris & Horn, 1991) failed to show such currents in neurons of the mollusk *Lymnaea stagnalis*, although they were detected at the single-channel level. The G292 osteoblast membrane was typically quite fragile, and attempts to prod the membrane or apply positive pressure to stretch the membrane during whole-cell recording were invariably unsuccessful. As an alternative approach to stretching the cell's membrane directly, the osmolarity of the bath was lowered to produce cell swelling. The underlying assumption was that the predominant current evoked after hypotonic shock would be mediated by the maxi-K^+ channel. That is, decreasing the extracellular osmolarity would produce an increase in the amplitude of the evoked outward current.

Typically, whole-cell recordings were made in isotonic ECS, and were followed by recordings in either hypotonic ECS or a reduced-salt isotonic solution (reduced ECS). The latter solution, which was isotonic to the cell, served as a control for changes in the electrochemical gradient for sodium and potassium in hypotonic ECS.

Overall, a total of 23 cells was studied for the effects of hypotonic shock, and in virtually every case there was an increase in the outward current after reducing the osmolarity of the bath. About a third of the cells, however, did not recover from the initial hypotonic perfusion. That is, once tested for the effects of hypotonic shock, after replacing isotonic ECS in the bath, the amplitude of evoked currents did not return to baseline levels and the physical appearance of the cells was visibly altered, suggesting irreversible damage. Accordingly, only those cells which demonstrated at least 50% recovery were included in the analysis. Of these cells, the vast majority (14/15) responded to hypotonic shock with an increase in the amplitude and a decrease in the rise time of the evoked current. The onset of these effects was noticeable within <1 min of replacing the bath, and reached a steady state within 3–4 min in most (73%; 11/15) of cells tested.

In the example shown in Fig. 8, in isotonic ECS, voltage steps ranging from ~50 to 150 mV elicited a high-conductance, outwardly rectifying current in G292 cells (Fig. 8*A*; left panel). Reducing the osmolarity of the bath (middle panel) resulted in a ~2-fold increase in the amplitude of the evoked current and a reduction of the rise time. By contrast, in reduced-salt isotonic ECS (right panel), there was a small, albeit nonsignificant (*see below*), increase in peak current and negligible changes in rise time. In this example, at a membrane potential of 150 mV, substituting hypotonic for isotonic ECS increased the peak current from 2.1 to 3.9 nA, and decreased the rise time from 4.5 to 2.1 msec; in reduced ECS, peak current was 2.5 nA and rise time was 4.2 msec. Fig. 8*B* illustrates the current- and conductance-voltage relationships for the current traces in Fig. 8*A*.

To quantify the effects of hypotonic shock, slope conductances for the linear portion (90–150 mV) of the *I-V* relationships were compared among a total of nine cells tested with isotonic, hypotonic, and reduced-isotonic bath. In isotonic or reduced-isotonic medium, conductances did not differ significantly. In isotonic bath, mean conductance was 53.4 ± 8.7 nS (mean ± SEM; $n = 9$) *vs.* 58.71 ± 6.84 nS in reduced-isotonic bath (paired t-test; $P > 0.20$). By contrast, in hypotonic medium, there was a sig-

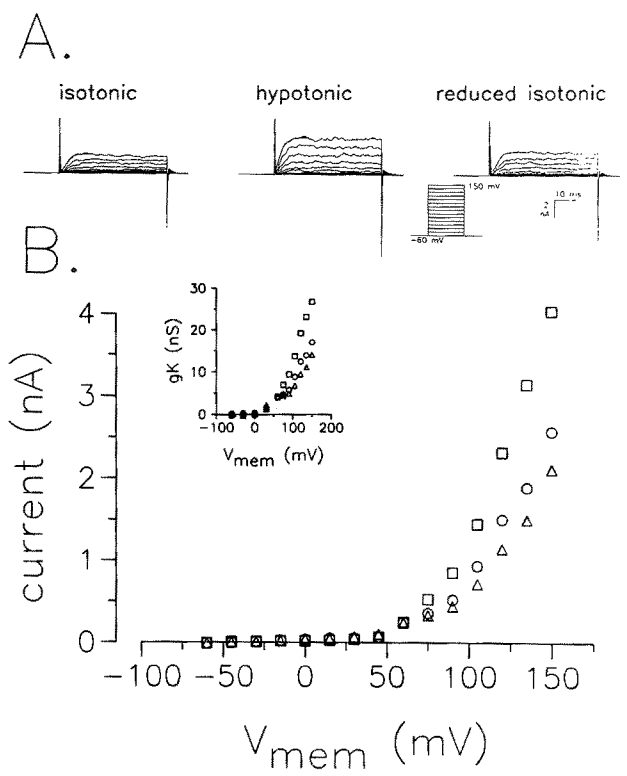

Fig. 8. (*A*) Whole-cell currents elicited by depolarizing voltage steps from a holding potential of −60 mV to the values indicated. Pulse duration was 50 msec. In isotonic ECS, positive potentials greater than 50 mV evoked a high-conductance, outwardly rectifying current (left panel). Exposure of the cell to hypotonic ECS (middle panel) increased the amplitude and rise time of the evoked currents, whereas perfusion with reduced-salt isotonic ECS (right panel) only slightly altered these values (*see text*). Time constants at 150 mV were fitted to the first 15 msec of the pulse, and are represented by solid lines in each trace. (*B*) Current-voltage relationships for the records in *A*. Inset: conductance-voltage relationships for these records, where $gK = I_K/V_{mem}$. Isotonic ECS (triangles); hypotonic ECS (squares); reduced-salt isotonic ECS (circles). Pipette: Ca^{2+}-free ICS. Three-day culture. C_{mem} was 4.8 pF and R_{series} was 17 MΩ, with 80% compensation. Leak currents were uncorrected.

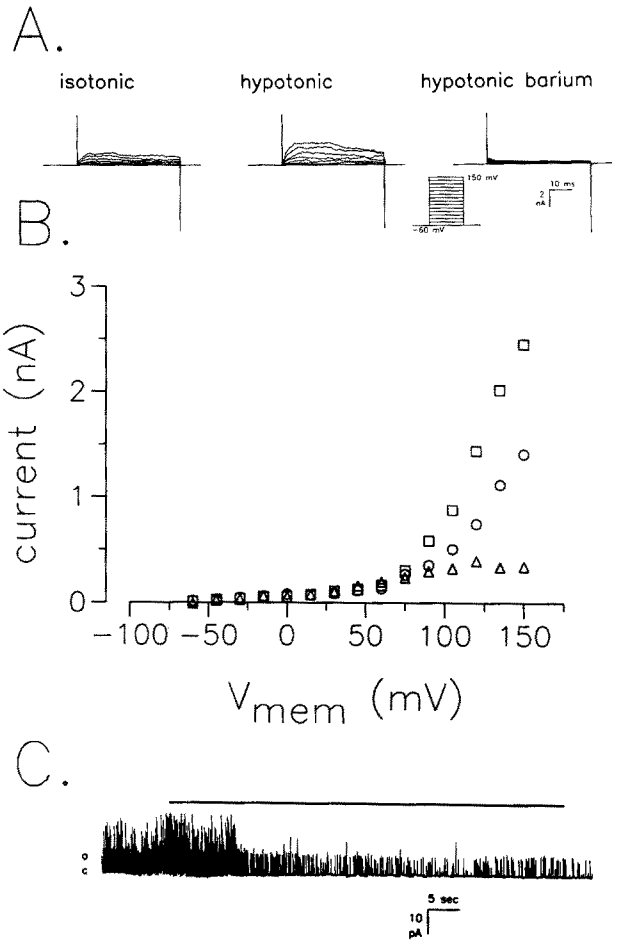

Fig. 9. Barium blockade of the outwardly rectifying current. (*A*) Outward currents activated by depolarization (as above) in isotonic ECS (left panel), hypotonic ECS (middle panel), and a hypotonic barium salt solution (right panel). (*B*) Current-voltage relationships for records in *A*. Isotonic ECS (circles); hypotonic ECS (squares); hypotonic barium (triangles). (*C*) Effect of barium on P_{open} of the maxi-K$^+$ channel in an excised, outside-out patch formed after the whole-cell records were obtained. The patch was formed in isotonic ECS and then perfused with the barium solution. The solid line above the trace approximates the onset of barium perfusion. Pipette: Ca^{2+}-free ICS; Membrane potential: 20 mV. The cell had been cultured for two days. C_{mem} was 4.2 pF and R_{series} was 19 MΩ, with 80% compensation. Leak currents were uncorrected.

nificant increase in the conductance to 71.6 ± 4.5 nS ($P < 0.03$).

The Macroscopic Current is Mediated by Potassium

Potassium selectivity of the outwardly rectifying current was confirmed in two ways: First, the current persisted in the acetate salt (*data not shown*). Second, in each case tested ($n = 6$), the current was effectively blocked by barium. In the example shown in Fig. 9*A*, when the cell was perfused with hypotonic ECS (middle panel), as expected, there was a ~2-fold increase in the outward current. This current was virtually eliminated after an equivalent hypotonic solution containing barium was substituted in the bath (right panel). Fig. 9*B* shows the current-voltage relationship derived from these records. That barium was capable of blocking the maxi-K$^+$ channel was confirmed at the single-channel level. The record in Fig. 9*C* was obtained from an excised, outside-out patch formed after the whole-cell currents illustrated in Fig. 9*A* were re-

corded, and clearly shows the effect of barium on the activity of the large-conductance channel. In this case, barium reduced P_{open} about tenfold, from 0.22 in ECS to 0.02 in the barium solution.

Discussion

There were two major findings in this study. First, the predominant cation conductance in G292 osteoblastic cells has been identified. This K^+-selective channel was both voltage gated and calcium dependent, and showed kinetic properties that classified it as one of the maxi-K^+ channels found in many cell types. Second, it has been shown that this channel was also sensitive to mechanical stretch.

Comparison with other Maxi-K^+ Channels

Qualitatively, the maxi-K^+ channel in G292 osteoblastic resembled the "classical" $K_{(Ca)}$ channel found in a wide variety of nonosteogenic cells, both excitable and nonexcitable (Magleby & Pallotta, 1983*a*, *b*; Gallin, 1984; Bolivar & Cereijido, 1987). Characteristic features that are shared by these channels are (i) relatively large conductances (*ca.* 150–250 pS), (ii) voltage sensitivity, and (iii) calcium dependence. Moreover, the kinetic behavior of these channels is similar insofar as changes in voltage and/or calcium levels affect both burst and interburst intervals (Magleby & Pallotta, 1983*b*). Thus, in essentially all respects, the 160 pS K^+-selective channel in G292 cells fits the criteria for this class of ion channel. Indeed, the apparent rectification properties of the channel, as well as the increase in its conductance in symmetric solutions of ICS (Fig. 1*B*), was also characteristic of large-amplitude, Ca-activated K^+ channels (Singer & Walsh, 1984; Ravesloot et al., 1990).

There was one minor difference between its behavior and that of $K_{(Ca)}$ channels found in osteogenic cells from primary cultures of chick calvaria. In whole-cell recordings from avian cells, the outwardly rectifying current showed a higher degree of variability in amplitude than was seen in G292 cells (*see* Fig. 2: Ravesloot et al., 1990). This difference may have been due to the heterogeneity of the primary culture cell population itself, or the effect of coculturing a variety of osteogenic cells which may interact metabolically.

Comparison with other Large-Amplitude Mechanosensitive Channels

Our previous studies showed that membrane stretch in G292 cells affected burst and interburst durations of the 160 pS channel (Davidson et al., 1990). Since this was similar to calcium effects on the kinetic behavior of $K_{(Ca)}$ channels (Fig. 6*B*), it raised the possibility that calcium, rather than membrane tension, modulated channel activity. Given its amplitude and conductance properties, we suggested that this channel might be a $K_{(Ca)}$ conductance, although there was no direct evidence for voltage or calcium dependency. Indeed, recent studies of other "stretch-activated" maxi-K^+ ion channels have shown that a $K_{(Ca)}$ conductance is activated during membrane stretch as a result of calcium influx. In opossum kidney cells (Ubl et al., 1988), hypotonic shock induces channel activity that is calcium dependent and mimicked by the ionophore A23187, while in rabbit MTAL cells both hypotonic shock and applied negative pressure (in the presence of calcium) activate a maxi-K^+ conductance (Taniguchi & Guggino, 1989). In the present experiments using excised patches, changes in internal calcium could not have been a significant factor. Thus, G292 cells exhibit a pressure-dependent increase in P_{open}, which appears to result from an increase in burst duration coupled with a decrease in the interburst interval (Fig. 7). It is possible that the 40% decrease in pressure sensitivity in excised ($0.18/cm^2$) *vs.* cell-attached ($0.29/cm^2$) patches may reflect the contribution of increased calcium levels during membrane stretch in the cell-attached configuration. Indeed, with Ca^{2+}-free ICS in the pipette, the rate of channel activity in the outside-out patch in Fig. 9*C* following hypotonic shock (Fig. 9*A*; middle panel) was surprisingly elevated ($P_{open} \sim 0.20$). This may have resulted from a slowly reversing (or irreversible) distension of stretch-sensitive channels. As noted above, in a number of excised patches the channel showed variability in its response to subsequent stretch following initial membrane distension. Thus, following cell swelling, the channel's spontaneous activity might have increased. Further, to form the outside-out patch the cell membrane was ruptured, allowing some exchange between the bath (pCa5) and internal solution. This alone may have elevated internal calcium levels enough to sustain channel activity.

Is There More Than One Population of Maxi-K^+ Channel?

That P_{max} (Eq. (4)) of the channel averaged *ca.* 50% may be interpreted in several ways: Since the membrane could not withstand negative pressures in excess of -4 to -5 cm Hg, it was possible that the channel was not activated maximally. This is unlikely, however, since curve-fits with P_{max} greater than 0.60 consistently increased the variance of the

pressure-sensitivity curve (Fig. 4*B*). More likely, either the channel may have inherent limitations in terms of activation by membrane tension, i.e., may plateau, or membrane tension may not affect all the channels in a patch equally (*see below*). It is possible that mechanosensitive $K_{(Ca)}$ channels may represent only a subset of a larger population of $K_{(Ca)}$ channels. In a number of cases it was impossible to modulate the activity of the $K_{(Ca)}$ channel with negative pressures exceeding -4 cm Hg, suggesting the existence of stretch-insensitive $K_{(Ca)}$ channels.

Physiological Role

One likely role of the maxi-K^+ channel is to modulate V_{mem} during mechanical loading of the cell. In vitro, bone cells respond to mechanical stress with elevated levels of cyclic-AMP (Rodan et al., 1975) and inositol phosphates (Sandy et al., 1989), probably due to mobilization of second messenger pathways activated by the phospholipases (Sandy & Farndale, 1991). One result may be depolarization of the cell. The present findings suggest that the ability of the maxi-K^+ channel to counter the depolarizing effects of calcium and/or modulate other voltage-dependent conductances during mechanical perturbation is enhanced by its mechanosensitive properties. An additional role for this channel may be related to cell volume regulation. In several cell types, including bone cells, hypotonic shock induces a calcium-dependent hyperpolarization of the cell membrane (Ubl et al., 1988; Taniguchi & Guggino, 1989; Yamaguchi et al., 1989). The hyperpolarizing effects of membrane stretch are thought to be due to the activation of a large-conductance Ca^{2+}-dependent K^+ current resulting from an increase in internal calcium via stretch-sensitive calcium channels. In the present experiments, a more direct effect of mechanical stretch on these K^+ channels has been demonstrated at the single channel level. In whole-cell recordings, the existence of a macroscopic current evoked by hypotonic shock suggests that the stretch-induced hyperpolarizing response in G292 cells may be linked to cell volume regulation, and may be augmented by the intrinsic mechanosensitive properties of its maxi-K^+ channel.

In summary, in both excised-patch and whole-cell recordings, G292 osteoblastic cells have been shown to contain a class of large conductance, calcium-activated K^+ channels that are also sensitive to membrane stretch. This finding suggests that a hyperpolarizing current, mediated in part by these channels, may be associated with early events during mechanical loading of bone cells. While many cells contain the maxi-K^+ channel, thus far intrinsic mechanosensitive properties have not been reported. In G292 osteoblastic cells, at least one population of this class of ion channel is sensitive to membrane tension, and may represent a unique adaptation of the bone cell membrane to mechanical stress.

This work was supported by NIH grant DE09662. I thank Jill London, Barbara Ehrlich, and Stephen Sims for helpful comments on the manuscript.

References

Bolivar, J.J., Cereijido, M. 1987. Voltage and Ca^{2+}-activated K^+ channel in cultured epithelial cells (MDCK). *J. Membrane Biol.* **97:**43–51

Chesnoy-Marchais, D., Fritsch, J. 1989. Chloride current activated by cyclic AMP and parathyroid hormone in rat osteoblasts. *Pfluegers Arch.* **415:**104–114

Chow, S.Y., Chow, Y.C., Jee, W.S.S., Woodbury, D.M. 1984. Electrophysiological properties of osteoblastlike cells from the cortical endosteal surface of rabbit long bones. *Calcif. Tissue Int.* **36:**401–408

Davidson, R.M., Tatakis, D.N., Auerbach, A. 1990. Multiple forms of mechanosensitive ion channels in osteoblast-like cells. *Pfluegers Arch.*, **416:**646–651

Dixon, S.J., Aubin, J.E., Dainty, J. 1984. Electrophysiology of a clonal osteoblast-like cell line: Evidence for the existence of a Ca^{2+}-activated conductance. *J. Membrane Biol.* **80:**49–58

Duncan, R., Misler, S. 1989. Voltage-activated and stretch-activated Ba^{2+} conducting channels in an osteoblast-like cell line (UMR 106). *FEBS Lett.* **251:**17–21

Edelman, A., Fritsch, J., Balsan, S. 1986. Short-term effects of PTH on cultured rat osteoblasts: changes in membrane potential. *Am. J. Physiol.* **251:**C483–490

Ferrier, J., Ward, A. 1986. Electrophysiological differences between bone cell clones: Membrane potential responses to parathyroid hormone and correlation with the cAMP response. *J. Cell. Physiol.* **126:**237–242

Fritsch, J., Edelman, A., Balsan, S. 1988. Early effects of parathyroid hormone on membrane potential of rat osteoblasts in culture: Role of cAMP and Ca^{2+}. *J. Bone Mineral Res.* **3:**547–554

Gallin, E. 1984. Calcium- and voltage-activated potassium channels in human macrophages. *Biophys. J.* **46:**821–825

Hamill, O.P., Marty, A., Neher, E., Sakmann, B., Sigworth, F. 1981. Improved patch-clamp techniques for high resolution current recording from cells and cell-free membrane patches. *Pfluegers Arch.* **391:**85–100

Heath, J.C., Meikle, M.C., Atkinson, S.J., Reynolds, J.J. 1984*a*. A factor synthesized by rabbit periosteal fibroblasts stimulates bone resorption and collagenase production by connective tissue cell in vitro. *Biochim. Biophys. Acta* **800:**301–305

Heath, J.C., Atkinson, S.J., Meikle, M.C., Reynolds, J.J. 1984*b*. Mouse osteoblasts synthesize collagenase in response to bone resorbing agents. *Biochim. Biophys. Acta* **802:**151–154

Magleby, K.L., Pallotta, B.S. 1983*a*. Calcium dependence of open and shut intervals distributions from calcium-activated potassium channels in cultured rat muscle. *J. Physiol.* **344:**585–604

Magleby, K.L., Pallotta, B.S. 1983*b*. Burst kinetics of single

calcium-activated potassium channels in cultured rat muscle. *J. Physiol.* **344:**605–623

Morris, C.E., Horn, R. 1991. Failure to elicit neuronal macroscopic mechanosensitive currents anticipated by single channel studies. *Science* **251:**1246–1248

Ngan, P.W., Crock, B., Varghese, J., Lanese, R., Shanfield, J., Davidovitch, Z. 1988. Immunohistochemical assessment of the effect of chemical and mechanical stimuli on cAMP and prostaglandin E levels in human gingival fibroblasts in vitro. *Arch. Oral Biol.* **33:**163–174

Peebles, P.T., Trisch, T., Papageorge, A.G. 1978. Isolation of four unusual pediatric solid tumor cell lines. *Pediatric Res.* **12:**485(#727)

Pollack, S.R., Salzstein, R., Pienkowski, D. 1984. The electric double layer in bone and its influence on stress-generated potentials. *Calcif. Tissue Int.* **36:**S77

Ravesloot, J.H., Van Houten, R.J., Ypey, D.L., Nijweide, P.J. 1990. Identification of Ca^{2+}-activated K^+ channels in cells of embryonic chick osteoblast cultures. *J. Bone Mineral Res.* **5:**1201–1210

Ravesloot, J.H., Van Houten, R.J., Ypey, D.L., Nijweide, P.J. 1991. High-conductance anion channels in embryonic chick osteogenic cells. *J. Bone Mineral Res.* **6:**355–364

Rodan, G. 1991. Perspectives: Mechanical loading, estrogen deficiency, and the coupling of bone formation to bone resorption. *J. Bone Mineral Res.* **6:**527–530

Rodan, G.A., Burrette, C.A., Harvey, A., Mensi, T. 1975. Cyclic AMP and cyclic GMP: Mediators of the mechanical effects of bone remodeling. *Science* **189:**467–469

Sackin, H. 1989. A stretch-activated K^+ channel sensitive to cell volume. *Proc. Natl. Acad. Sci. USA* **86:**1731–1735

Sandy, J.R., Farndale, R.W. 1991. Second messengers: regulators of mechanically-induced tissue remodeling. *Eur. J. Orthodont.* **13:**271–278

Sandy, J.R., Meghji, S., Farndale, R.W., Meikle, M.C. 1989. Dual elevation of cyclic AMP and inositol phosphates in response to mechanical deformation of murine osteoblasts. *Biochim. Biophys. Acta* **1010:**265–269

Shupnik, M.A., Tashjian, A.H., Jr. 1982. Epidermal growth factors and phorbol ester actions on human osteosarcoma cells: Characterization of responsive and nonresponsive cell lines. *J. Biol. Chem.* **257:**12161–12164

Singer, J.J., Walsh, J.V. 1984. Large conductance Ca^{2+}-activated K^+ channels in smooth muscle cell membrane. *Biophys. J.* **45:**68–70

Snowdowne, K.W. 1987. The effects of stretch on sarcoplasmic free calcium of frog skeletal muscle at rest. *Biochim. Biophys. Acta* **862:**441–444

Taniguchi, J., Guggino, W.B. 1989. Membrane stretch: a physiological stimulator of Ca^{2+}-activated K^+ channels in thick ascending limb. *Am. J. Physiol.* **257:**F347–F352

Ubl, J., Murer, H., Kolb, H.-A. 1988. Hypotonic shock evoked opening of Ca^{2+}-activated K^+ channels in opossum kidney cells. *Pfluegers Arch.* **412:**551–553

Yamaguchi, D.T., Green, J., Kleeman, C.R., Muallem, S. 1989. Characterization of volume-sensitive, calcium-permeating pathways in the osteosarcoma cell line UMR-106-01. *J. Biol. Chem.* **264:**4383–4390

Yang, X. 1989. Characterization of Stretch-Activated Ion Channels in *Xenopus* Oocytes. Ph.D. Thesis. University of Buffalo, Buffalo

Ypey, D.L., Ravesloot, J.H., Buisman, H.P., Nijweide, P.J. 1988. Voltage-activated ionic channels and conductances in embryonic chick osteoblast cultures. *J. Membrane Biol.* **101:**141–150

Received 30 March 1992; revised 7 August 1992